Optical Fiber Technology 20 (2014) 615–620

Contents lists available at ScienceDirect

Optical Fiber Technology

www.elsevier.com/locate/yofte

Invited Paper

Mode-locked fiber lasers with significant variability of generation regimes

S. Kobtsev [a], S. Smirnov [a], S. Kukarin [a], S. Turitsyn [a,b,*]

[a] Division of Laser Physics and Innovation Technologies, Novosibirsk State University, 630090 Novosibirsk, Russia
[b] Aston Institute of Photonic Technologies, Aston University, Birmingham, B4 7ET Birmingham, UK

ARTICLE INFO

Article history:
Available online 29 August 2014

Keywords:
Fiber laser
Passively mode-locked laser
Ultrafast laser
Non-linear polarization evolution

ABSTRACT

We demonstrate a great variability of single-pulse (with only one pulse/wave-packet traveling along the cavity) generation regimes in fiber lasers passively mode-locked by non-linear polarization evolution (NPE) effect. Combining extensive numerical modeling and experimental studies, we identify multiple very distinct lasing regimes with a rich variety of dynamic behavior and a remarkably broad spread of key parameters (by an order of magnitude and more) of the generated pulses. Such a broad range of variability of possible lasing regimes necessitates developing techniques for control/adjustment of such key pulse parameters as duration, radiation spectrum, and the shape of the auto-correlation function. From a practical view point, availability of pulses/wave-packets with such different characteristics from the same laser makes it imperative to develop variability-aware designs with control techniques and methods to select appropriate application-oriented regimes.

1. Introduction

Mode-locked fiber lasers are widely used as sources of ultrashort optical pulses [1–6]. The growing use of fiber lasers for this purpose is supported by customer demand for reliable femto- and pico-second lasers with a long (or, better, unlimited) operation lifetime and without any need for manual adjustments. Fiber lasers mode-locked due to non-linear polarization evolution (NPE) may satisfy these requirements [7,8] as they make direct use of their resonators' non-linear properties and are able to generate pulses with durations as short as 50 fs and even less [9,10]. Being at the same time a promising tool and a unique platform for observing spectacular non-linear optical interactions, NPE mode-locked fiber lasers attract much attention from both scientists and laser engineers. Such lasers support a large variety of generation regimes [11], including pulses of different shapes [12–15], multi-pulse lasing at different fundamental repetition frequency multiples [16], as well as complex soliton structures [14,16] and soliton rains [17]. In the present work, we limit our analysis to single-pulse lasing, that is, when only one laser pulse/wave-packet is present over a single round trip of the cavity. However, as our results show, even within such a limited case, a large variety of lasing regimes is found, which may considerably (up to an order of magnitude or even more) differ from each other in pulse energy, duration, bandwidth, etc., and may dramatically differ from each other in pulse structure being either "conventional" (single-scale) smooth pulses or double-scale pulses (wave-packets) with complex internal structure and phase fluctuations [18]. This has an important practical impact, calling for a variability-aware design of laser systems with embedded control techniques and methods to select appropriate output pulses.

2. Experimental setup

The setup used in our experiments is similar to those described in our previous studies [18–20], see Fig. 1. The fiber laser has a ring cavity with a wave-division-multiplexing (WDM) used to couple in the pump radiation. Either 2 m-long Er- or 8 m-long Yb-doped optical fiber is used in different experiments as the active medium, both of which produce qualitatively similar results at net-normal and all-normal cavity dispersion respectively. Either SMF-28 or normal-dispersion fiber (NDF) is used to elongate the cavity and thus increase pulse energy. Output laser radiation is extracted through a fiber polarization beam splitter (FPBS) or through an additional coupler inserted into the cavity. Mode-locked operation was achieved by adjusting fiber polarization controllers PC1, 2. Operation regimes were studied with the help of a fast oscilloscope, an optical spectrum analyzer (OSA), and an optical pulse auto-correlator.

* Corresponding author at: Division of Laser Physics and Innovation Technologies, Novosibirsk State University, 630090, Novosibirsk, Russia. Fax: +7 (383)3634265.
E-mail address: kobtsev@lab.nsu.ru (S. Kobtsev).

http://dx.doi.org/10.1016/j.yofte.2014.07.009
1068-5200/

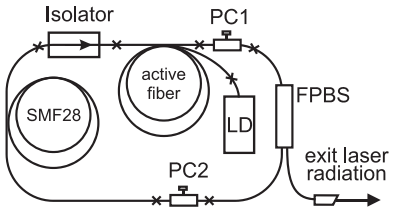

Fig. 1. Laser layout used in experiments. LD—laser diode, FPBS—fiber polarization beam splitter, PC1, 2—fiber polarization controllers.

3. Numerical model

In order to investigate the variety of possible single-pulse lasing regimes and their properties, we used a well-established numerical model based on a set of modified, non-linear Schrödinger equations for orthogonal polarization components of the field envelope [21]:

$$\frac{\partial A_x}{\partial z} = i\gamma\left\{|A_x|^2 A_x + \frac{2}{3}|A_y|^2 A_x + \frac{1}{3}A_y^2 A_x^*\right\} + \frac{g_0/2}{1 + E/(P_{sat}\cdot\tau)}A_x - \frac{i}{2}\beta_2 \cdot \frac{\partial^2 A_x}{\partial t^2} \quad (1)$$

$$\frac{\partial A_y}{\partial z} = i\gamma\left\{|A_y|^2 A_y + \frac{2}{3}|A_x|^2 A_y + \frac{1}{3}A_x^2 A_y^*\right\} + \frac{g_0/2}{1 + E/(P_{sat}\cdot\tau)}A_y - \frac{i}{2}\beta_2 \cdot \frac{\partial^2 A_y}{\partial t^2} \quad (2)$$

where A_x, and A_y are the orthogonal components of the field envelope, z is the longitudinal coordinate, t – time, $\gamma = 4.7 \times 10^{-5}$ $(\mathrm{cm\,W})^{-1}$, $\beta_2 = 23$ $\mathrm{ps^2/km}$ – non-linear and dispersion coefficients, $g_0 = 540$ dB/km – unsaturated gain coefficient, $P_{sat} = 52$ mW – saturation power for the active fiber. In order to accelerate simulations and spare computational resources, we reduced cavity length to 10 m, which corresponds to cavity round-trip time $\tau = 48$ ns. Similarly to [18,19], we integrated Eqs. (1) and (2) over 10^4 round-trips, using white noise as the initial condition for the first iteration. The term proportional to g_0 describes saturated optical gain and therefore was omitted while simulating pulse propagation in a passive fiber. Polarization controllers were taken into account through applying unitary matrices. Eqs. (1) and (2) were integrated numerically using step-split Fourier method. We checked carefully that the main results of this paper were not influenced by variation of numerical integration step, step number, mesh width, and number of mesh points, provided that these parameters were chosen in proper limits.

4. Results and discussion

The laser layout depicted in Fig. 1 includes two fiber polarization controllers, which provide several degrees of freedom, including the ability to trigger mode-locked operation and then switch between different generation regimes or adjust laser parameters. Since investigating lasing properties in multi-dimensional space is quite complicated, we confined ourselves to statistical study of different generation regimes. The approach consisted of choosing the polarization controller settings (tilt/slew angles) in a random way and integrating Eqs. (1) and (2) with white noise as the initial conditions. After a certain number (typically $10^3 \ldots 10^4$) of round-trips, we may obtain one of the following solutions: (i) quasi-CW laser operation (no mode-lock reached; thus Eqs. (1) and (2) and their numerical solution are not valid); (ii) multi-pulse mode-locked operation (that is, two or more pulses co-exist in the cavity); and (iii) single-pulse, mode-locked operation. If a single-pulse, mode-locked operation is reached after the fixed amount of cavity round-trips, the program saves the results (tilt angles of PC1, 2, pulse duration, energy, optical spectrum, temporal intensity distribution, etc.). Otherwise, no information is kept about this program run. In either case, the program selects a new combination of random PC settings and proceeds with the next run, thus accumulating information about single-pulse operation regimes.

The lasing regimes found in simulation demonstrate both quantitative and qualitative differences. Qualitatively, one can distinguish two main types of single-pulse generation regimes: fully coherent, single-scale, and double-scale pulses with complex inner structure [19]. Temporal distribution of radiation intensity for fully coherent pulses features a smooth envelope and can be described by a single parameter, that is, the envelope width (single-scale or "conventional" pulses). In contrast, temporal intensity distribution of the radiation of partially coherent pulses is stochastic: inside wave-packets with overall duration of several picoseconds to several nanoseconds; there are fast stochastic variations of radiation intensity with typical time scale of a hundred to several hundred femtoseconds.

Correspondingly, temporal distribution of radiation intensity for such pulses (wave-packets or double-scale pulses) is defined by two temporal parameters: the pulse-train envelope width and the typical intensity fluctuation time inside the train. Overall parameters of the entire wave packet, such as bandwidth, energy, and duration, fluctuate around their average values within a big range from one packet to another. Intensity fluctuations inside single wave-packets may also vary from relatively small values up to peak wave-packet intensity. Lasing regimes with strong intensity fluctuations are usually classified as noise-like generation.

Double-scale pulses have not yet received a universal designation. Different terms are found across the available literature: noise-like pulses [22,23], double-scale lumps [19], femtosecond clusters [24], etc. This type of pulse can be easily identified by a singular auto-correlation function shape featuring a narrow (100–200 fs) peak on a broader picosecond pedestal. Significant attention to these pulses is predominantly due to the presence of femtosecond components with high peak power, while the cavities of fiber lasers generating them may have relatively large dispersion.

There is also a series of intermediate possibilities between "conventional" laser pulses and noise-like generation which manifests a relatively small and variable fraction of intensity noise and phase fluctuations on the background of single-scale laser pulses [18]. Remarkably, even inside a single type of lasing (for example, single-scale or double-scale pulses), the studied laser supports a large variety of sub-regimes that correspond to different settings of PC1, 2 and thus differ vis-à-vis energy, duration, bandwidth, etc. Generated pulse parameters may vary by an order of magnitude or even more, depending on PC settings. Probability density functions (PDF) for rms-bandwidth (see Fig. 2(a) and (b)) and rms-duration (see Fig. 2(c) and (d)) obtained by randomly changing simulation PC settings are shown in Fig. 2. These PDFs reveal the extent of parameter variability in different realizations of two main single-pulse lasing regimes, namely conventional lasing (Fig. 2(a) and (c)) and double-scale pulse generation (Fig. 2(b) and (d)). For instance, rms-bandwidth varied in random simulation runs from 0.2 up to 3.9 nm for single-scale pulses and from 0.3 up to 7.4 nm for double-scale pulses being a function of PC settings. (Note that given values are pulse rms-bandwidth, which is usually several times as narrow as the spectrum's full width at half-maximum, FWHM. As an example, for Π-shaped spectrum, the ratio between spectral FWHM and rms-bandwidth is 3.5. For differently shaped spectra, this ratio may vary).

Another important difference between lasing regimes attainable at different angular settings of intra-cavity PCs is related to

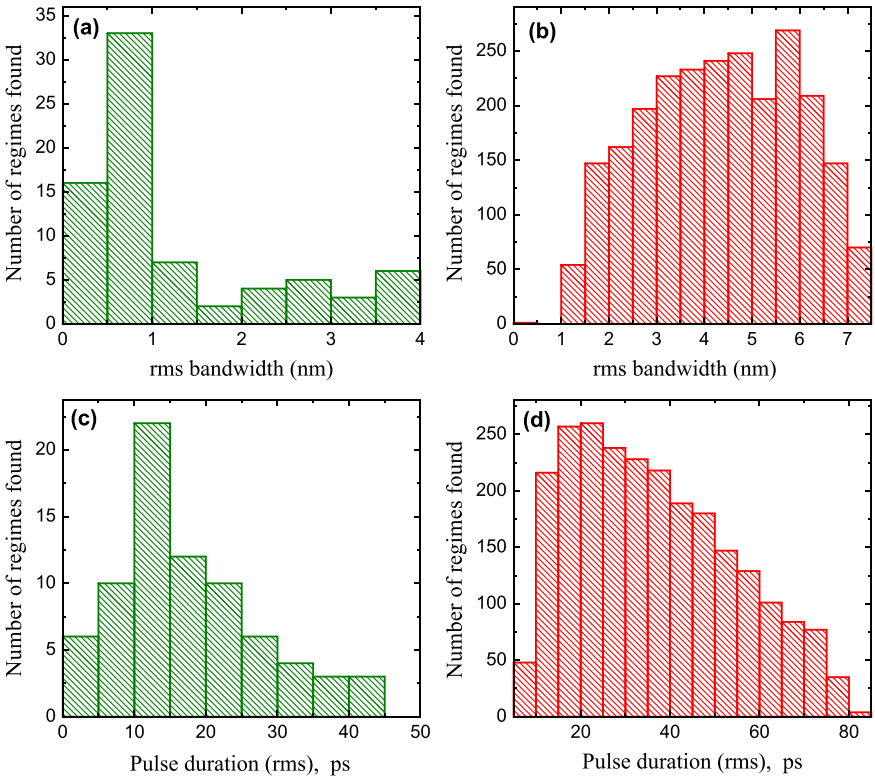

Fig. 2. Rms bandwidth (a, b) and rms-pulse duration (c, d) variability in simulated single-scale (a, c) and double-scale (b, d) single-pulse generation regimes.

efficiency of non-linear laser pulse conversion. Very recently it was found that efficiency of second harmonic generation (SHG) may vary by an order of magnitude or more depending, along with other laser pulse parameters, on PC settings (see [20] and Fig. 3(a and b)). In order to generalize our conclusions, we study dimension-relative SHG efficiency, which does not depend on pump power and thickness of the thin non-linear crystal, but is sensitive to mode correlations and fluctuations, thus allowing us to easily compare different lasing regimes from the viewpoint of efficiency of non-linear frequency conversion. It is defined [20] as the ratio of two SH powers, of which the first is obtained when the non-linear crystal is pumped by a laser pulse and the second is generated with single-mode monochromatic pumping of the same power. As our simulation shows, double-scale pulses have comparable or higher SHG-relative efficiency compared with that of single-scale laser pulses of the same duration, see Fig. 3(c).

We also conducted a comparative study of Raman scattering spectra generated by single-scale and double-scale laser pulses in a long stretch of extra-cavity fiber. As is illustrated below, notwithstanding similar duration of single-scale and double-scale pulse envelopes, Raman spectra resulting from these pulses are substantially different.

Shown in Figs. 4 and 5 are the radiation spectra and auto-correlation functions of single-scale and double-scale pulses studied in our experiment. Pulses of both types were generated in the laser cavity of Fig. 1 at different polarization controller positions. Auto-correlation functions were registered using commercial scanning auto-correlator "Tekhnoscan FS-PS-Auto" with working range of 5 fs to 35 ps. Certain noisiness of the recorded auto-correlation functions is due to a rather small fraction of the output radiation used for their measurement. Optical spectra were similarly registered by using a small amount of output power guided into

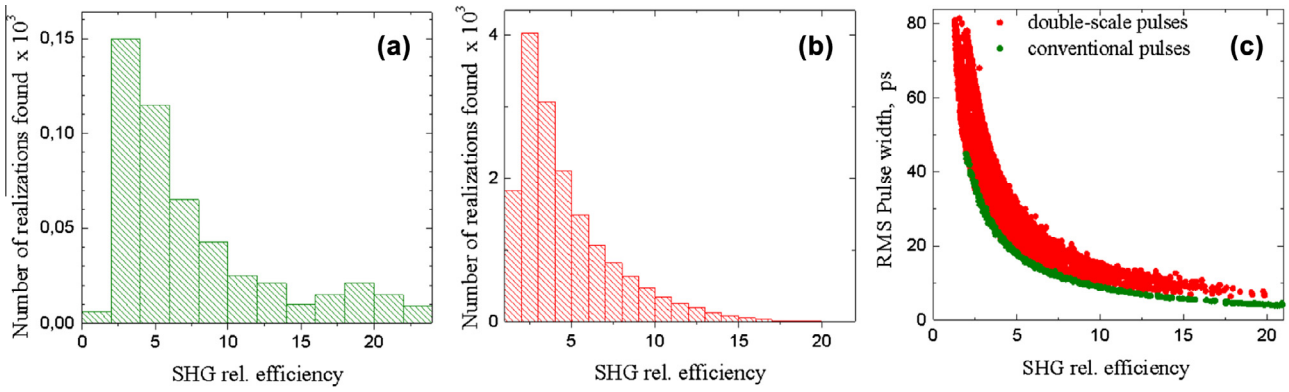

Fig. 3. Relative SHG efficiency in single-scale (a) and double-scale (b) single-pulse generation regimes and its correlation with rms pulse duration, ps (c).

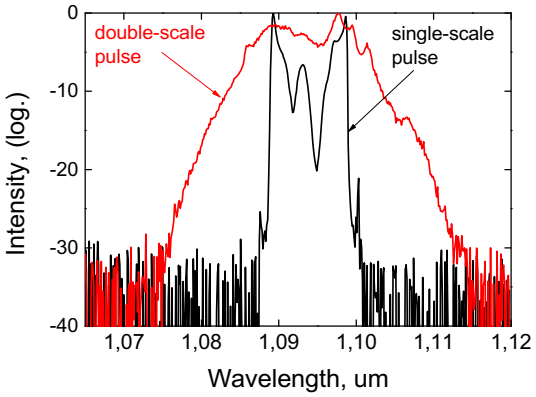

Fig. 4. Radiation spectra of single-scale (black curve) and double-scale (red curve) pulses used in the experiment. (For interpretation of the references to colour in this figure legend, the reader is referred to the web version of this article.)

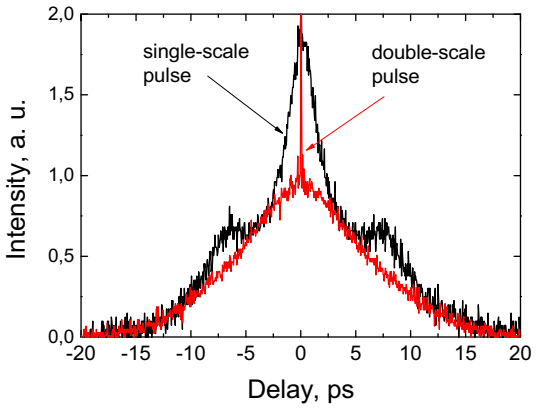

Fig. 5. Auto-correlation functions of single-scale (black curve) and double-scale (red curve) pulses used in the experiment. (For interpretation of the references to colour in this figure legend, the reader is referred to the web version of this article.)

an optical spectrum analyzer Advantest Q8381A. Both auto-correlation function and spectra of the generated pulses were measured in real time in order to know with certainty, which particular type of pulses is generated at a given moment. Mode locking was triggered by mutual adjustment of the polarisation controllers and pump radiation power within 1.3–1.5 W. Single-scale pulses have a Π-shaped optical spectrum and quasi bell-shaped auto-correlation function, whereas spectrum of double-scale pulses is much smoother and bell-shaped, and its ACF contains a narrow 180-fs long peak on a wide 12-ps long pedestal.

Fig. 6 shows Raman scattering spectra of single-scale (red curves) and double-scale (black curves) pulses propagating along a 1.2-km long phosphosilicate fiber. In order to produce sufficient spectral conversion, pulses from the reference fiber oscillator could be passed through a fiber optic amplifier to reach the average output power of 840 mW. This figure presents broader Raman scattering spectra of double-scale pulses in comparison to analogous spectra for single-scale pulses. Most likely, this is a result of femtosecond components present in the structure of double-scale pulses, which have higher non-linear conversion efficiency.

5. Ultra-long mode-locked fiber lasers: discussion

In the preceding sections, we have shown a great variety of generation regimes in NPE mode-locked fiber lasers instantiated by different settings of intra-cavity polarization controllers. By adjusting these settings, either manually or through automated

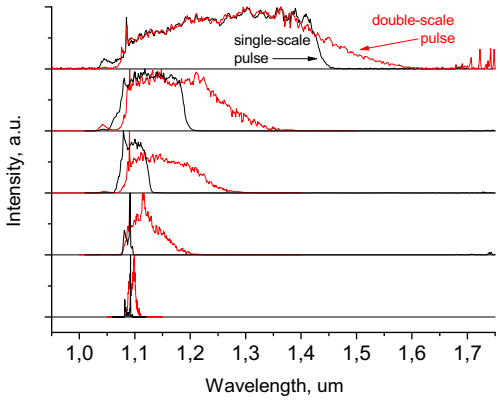

Fig. 6. Raman radiation spectra from 1.2-km long phosphosilicate fiber pumped with single-scale (black curves) and double-scale (red curves) pulses. (For interpretation of the references to colour in this figure legend, the reader is referred to the web version of this article.)

actuators, one can achieve switching between generation regimes and, consequently, significant changes in the generated laser pulse parameters. However, fiber lasers offer another important degree of freedom that can be used for designing novel generation regimes: resonator length. As was demonstrated by multiple groups [25–33], the cavity length has a substantial impact on the output pulse parameters in mode-locked fiber lasers. Specifically, it is possible to control the pulse energy and repetition rate by changing the laser cavity. Indeed, the pulse repetition rate ν_{rep} is inversely proportional to the laser cavity length L, $\nu_{rep} \sim c/(n \times L)$, where c/n is the speed of light inside the fiber cavity. The energy of a generated single pulse E at constant average output power P_{av} is inversely proportional to the pulse repetition rate, and, therefore, directly proportional to the cavity length: $E \sim (P_{av}/\nu_{rep}) \sim (P_{av} \times L \times n/c)$. Hence, it is possible to proportionally increase the pulse energy and reduce the repetition rate by laser cavity elongation.

It would be pertinent to note that this approach was earlier used in solid-state lasers [34]. However, for an open cavity containing discrete elements, the practical possibility of elongation is limited to approximately 100 m. Fiber lasers present a remarkable technical opportunity to increase length of resonant cavities. For instance, earlier publications reported passive mode-locking in 400 m long fiber lasers [35,36]. An important breakthrough in this field dates back to 2008 when mode-locked operation of a fiber laser with a 3.8 km cavity was achieved due to the effect of nonlinear polarization evolution of radiation [37]. At that time, the record high for mode-locked master oscillators pulse energy of 3.9 μJ was reported at a record low for this type of laser's pulse repetition rate of 77 kHz. The latter parameter was further reduced to 37 kHz [38] and to ~8 kHz [39], even though no improvement in pulse energy was achieved. Notwithstanding the respective elongation of the laser cavity to 8 and 25 km, the pulse energy remained unchanged at around 4 μJ. The existence of some upper limit to the pulse energy when the cavity of a mode-locked master oscillator is increased is the subject of the active current research [31] and is one of the field's important research challenges.

From the first experimental demonstration of high-energy pulse generation in ultra-long NPE mode-locked master oscillators [37], many research groups studied mode-locked fiber lasers with long and ultra-long resonators of different configurations. They demonstrated the possibility of passive mode locking in long cavities due to saturable absorbers, such as single-wall carbon nanotubes [25,40,41], semiconductor saturable absorber mirrors [42–44], and non-linear optical loop mirrors [45]. It was experimentally and theoretically confirmed that passively mode-locked fiber

master oscillators give rise to a broad variety of generation regimes in different cavity configurations [46–53], including generation of single and multiple pulses over a cavity round-trip, pulses with various duration, envelope shape, and spectrum width. The results of Refs [30,52] show that in ultra-long lasers, there is high probability of generating double-scale partially coherent pulses, whereas "normal" (single-scale) pulses with a smooth temporal optical phase shape and large chirp become difficult to obtain. This indicates a step difference from the traditional mode-locking theory and may be considered as a partial mode-locking, when phase locking is not between all resonator modes, but rather between groups/clusters of modes. Nevertheless, experimentally generating strongly chirped pulses in a 1 km laser cavity with mode-locking due to a carbon nanotube saturable absorber was reported in [25,40]. The paper [28] reports lasing in 1.4 km long Yb-doped fiber laser with steep spectral edges, which are attributed to a "conventional", stable, single-pulse generation regime [18,19].

Therefore, in principle, mode-locked fiber master oscillators with long and ultra-long cavities may be used to generate pulses with relatively high energies without any additional amplification or Q-switching, at the same time as they exhibit a broader variety of operation regimes compared to lasers with "short" resonators (on the order of several meters). In regimes with one pulse over the cavity round-trip, mode-locked fiber master oscillators can produce both fully and partially coherent pulses (double-scale wave-packets). Such systems require further analysis and numerical modeling.

The variety of generation regimes in mode-locked fiber master oscillators with long and ultra-long cavities, as well as significant variability of parameters of single-pulses/wave-packets produced therein, are of great interest both for fundamental research in laser physics and for practical applications of laser pulses with new unique parameters.

6. Conclusions

Our simulation and experiments demonstrate considerable spread of pulse parameters generated by fiber lasers mode-locked due to NPE. This finding should encourage users to carefully control at least the duration and optical spectrum of laser pulses, since the pulse parameters may change considerably, for example, due to relaxation of stress introduced by fiber polarization controllers, equivalent to a change in PC settings. This is of primary importance in the case of long and ultra-long fiber lasers, which are characterized by substantial length of non-linear interactions, which lead to considerable amplification of perturbations and make such lasers highly prone to undesired irregular regime hops. Note also that NPE mode-locked fiber lasers are relatively sensitive to ambient conditions because fiber birefringence depends on temperature, mechanical stress, and so on. Uncontrollable fiber birefringence changes make it necessary to adjust polarization controllers in order to trigger mode-locked operation or to stabilize it. Adjustment, however, may lead to the start of a mode-locked regime substantially different from the one before the adjustment.

Another important point of our study is that various lasing regimes should be carefully chosen in order to optimally meet the requirements of a particular laser application. Using second harmonic generation and Raman frequency conversion as a test bed, we have shown that different lasing regimes' efficiency may vary considerably even if laser pulses generated in different regimes have similar energies and duration.

The technological remedy (for example, in the form of control and adjustment elements) for the discussed output pulse characteristic variability should be incorporated into laser system designs.

Acknowledgments

This work was supported by the Marie Curie International Exchange Scheme, Research Executive Agency Grant "TelaSens" No 269271; ERC project ULTRALASER; Grants of Ministry of Education and Science of the Russian Federation (agreement No. 14.B25.31.0003; basic research order No. ZN-06-14 (2419); order No. 3.162.2014/K); Russian President Grant MK-4683.2013.2; Grant of SKOLKOVO Foundation (G-13-131); Council of the Russian President for the Leading Research Groups (project No. NSh-4447.2014.2).

References

[1] L.E. Nelson, D.J. Jones, K. Tamura, H.A. Haus, E.P. Ippen, Ultrashort-pulse fiber ring lasers, Appl. Phys. B 65 (1997) 277–294.
[2] A. Tünnermann, J. Limpert, S. Nolte, Ultrashort pulse fiber lasers and amplifiers, in: F. Dausinger, F. Lichtner, H. Lubatschowski (Eds.), Femtosecond Technology for Technical and Medical Applications, Topics in Applied Physics, vol. 96, Springer-Verlag, Berlin, Heidelberg, 2004, pp. 35–54.
[3] F.W. Wise, A. Chong, W.H. Renninger, High-energy femtosecond fiber lasers based on pulse propagation at normal dispersion, Laser Photonics Rev. 2 (2008) 58–73.
[4] J. Hecht, Fiber lasers bring femtoseconds to the masses, Laser Focus 1, 2010, http://www.laserfocusworld.com/articles/2010/01/fiber-lasers-bring.html.
[5] O.G. Okhotnikov (Ed.), Fiber Lasers, Wiley-VCH Verlag, Weinheim, 2012.
[6] M.E. Fermann, Mode locked fiber lasers, past, present and future. CLEO Technical Digest, OSA, 2012, CTu1I.5.pdf http://wr.lib.tsinghua.edu.cn/sites/default/files/CTu1I.5.pdf.
[7] V.J. Matsas, T.P. Newson, D.J. Richardson, D.N. Payne, Self-starting, passively mode-locked fiber ring soliton laser exploiting non-linear polarisation rotation, Electron. Lett. 28 (1992) 1391–1393.
[8] M. Hofer, M.H. Ober, F. Haberl, M.E. Fermann, Characterization of ultrashort pulse formation in passively mode-locked fiber lasers, IEEE J. Quantum Electron. 28 (1992) 720–728.
[9] F.Ö. Ilday, J.R. Buckley, H. Lim, F.W. Wise, W.G. Clark, Generation of 50-fs, 5-nJ pulses at 1.03 μm from a wave-breaking-free fiber laser, Opt. Lett. 28 (2003) 1365–1367.
[10] F. Ilday, J. Buckley, L. Kuznetsova, F. Wise, Generation of 36-femtosecond pulses from a ytterbium fiber laser, Opt. Express 11 (2003) 3550–3554.
[11] P. Grelu, N. Akhmediev, Dissipative solitons for mode-locked lasers, Nat. Photonics 6 (2012) 84–92.
[12] L.M. Zhao, D.Y. Tang, T.H. Cheng, C. Lu, Nanosecond square pulse generation in fiber lasers with normal dispersion, Opt. Commun. 272 (2007) 431–434.
[13] B. Ortaç, A. Hideur, M. Brunel, C. Chédot, J. Limpert, A. Tünnermann, F.Ö. Ilday, Generation of parabolic bound pulses from a Yb-fiber laser, Opt. Express 14 (2006) 6075–6083.
[14] J.M. Soto-Crespo, P. Grelu, N. Akhmediev, N. Devine, Soliton complexes in dissipative systems: vibrating, shaking, and mixed soliton pairs, Phys. Rev. E 75 (2007) 016613.
[15] W.H. Renninger, A. Chong, F.W. Wise, Pulse shaping and evolution in normal-dispersion mode-locked fiber lasers, IEEE J. Sel. Top. Quantum Electron. 18 (2012) 389–398.
[16] Ph. Grelu, J.M. Soto-Crespo, Temporal soliton "molecules" in mode-locked lasers: collisions, pulsations, and vibrations, Lect. Notes Phys. 751 (2008) 137–173.
[17] S. Chouli, P. Grelu, Rains of solitons in a fiber laser, Opt. Express 17 (2009) 11776–11781.
[18] S. Smirnov, S. Kobtsev, S. Kukarin, A. Ivanenko, Three key regimes of single pulse generation per round trip of all-normal-dispersion fiber lasers mode-locked with nonlinear polarization rotation, Opt. Express 20 (2012) 27447–27453.
[19] S. Kobtsev, S. Kukarin, S. Smirnov, S. Turitsyn, A. Latkin, Generation of double-scale femto/pico-second optical lumps in mode-locked fiber lasers, Opt. Express 17 (2009) 20707–20713.
[20] S. Smirnov, S. Kobtsev, S. Kukarin, Efficiency of non-linear frequency conversion of double-scale pico-femtosecond pulses of passively mode-locked fiber laser, Opt. Express 22 (2014) 1058–1064.
[21] G.P. Agrawal, Nonlinear fiber optics, third ed., Academic Press, 2001.
[22] M. Horowitz, Y. Barad, Y. Silberberg, Noise-like pulses with a broadband spectrum generated from an erbium-doped fiber laser, Opt. Lett. 22 (1997) 799–801.
[23] O. Pottiez, R. Grajales-Coutiño, B. Ibarra-Escamilla, E.A. Kuzin, J.C. Hernández-García, Adjustable noise-like pulses from a figure-eight fiber laser, Appl. Opt. 50 (2011) E24–E31.
[24] B. Nie, G. Parker, V.V. Lozovoy, M. Dantus, Energy scaling of Yb fiber oscillator producing clusters of femtosecond pulses, Opt. Eng. 53 (2014) 051505.
[25] E.J.R. Kelleher, J.C. Travers, E.P. Ippen, Z. Sun, A.C. Ferrari, S.V. Popov, J.R. Taylor, Generation and direct measurement of giant chirp in a passively mode-locked laser, Opt. Lett. 34 (2009) 3526–3528.
[26] S.V. Smirnov, S.M. Kobtsev, S.V. Kukarin, S.K. Turitsyn, Mode-locked fiber lasers with high-energy pulses, in: K. Jakubczak (Ed.), Laser Systems for Applications, InTech, Rijeka, Croatia, 2011, pp. 39–58.

[27] X. Li, X. Liu, X. Hu, L. Wang, H. Lu, Y. Wang, W. Zhao, Long-cavity passively mode-locked fiber ring laser with high-energy rectangular-shape pulses in anomalous dispersion regime, Opt. Lett. 35 (2010) 3249–3251.
[28] L.J. Kong, X.S. Xiao, C.X. Yang, Low-repetition-rate all-fiber all-normal-dispersion Yb-doped mode-locked fiber laser, Laser Phys. Lett. 7 (2010) 359.
[29] N. Li, J. Xue, C. Ouyang, K. Wu, J.H. Wong, S. Aditya, P.P. Shum, Cavity-length optimization for high energy pulse generation in a long cavity passively mode-locked all-fiber ring laser, Appl. Opt. 51 (2012) 3726–3730.
[30] I.A. Yarutkina, O.V. Shtyrina, M.P. Fedoruk, S.K. Turitsyn, Numerical modeling of fiber lasers with long and ultra-long ring cavity, Opt. Express 21 (2013) 12942–12950.
[31] C. Aguergaray, A. Runge, M. Erkintalo, N.G. Broderick, Raman-driven destabilization of mode-locked long cavity fiber lasers: fundamental limitations to energy scalability, Opt. Lett. 38 (2013) 2644–2646.
[32] T. Liu, D. Jia, J. Yang, J. Chen, Z. Wang, T. Yang, An ultra-long cavity passively mode-locked fiber laser based on nonlinear polarization rotation in a semiconductor optical amplifier, Laser Phys. 23 (2013) 095005.
[33] E.J.R. Kelleher, J.C. Travers, Chirped pulse formation dynamics in ultra-long mode-locked fiber lasers, Opt. Lett. 39 (2014) 1398–1401.
[34] V.Z. Kolev, M.J. Lederer, B. Luther-Davies, A.V. Rode, Passive mode locking of a Nd:YVO4 laser with an extra-long optical resonator, Opt. Lett. 28 (2003) 1275–1277.
[35] J.U. Kang Jr., R. Posey, Demonstration of supercontinuum generation in a long-cavity fiber ring laser, Opt. Lett. 23 (1998) 1375–1377.
[36] K.H. Fong, S.Y. Kim, K. Kazuro, H. Yaguchi, S.Y. Set, Generation of low-repetition rate high-energy picosecond pulses from a single-wall carbon nanotube mode-locked fiber laser, Optical Amplifiers and their Applications Conference (OAA 2006), Whistler, British Columbia, Canada, OMD4, June 2006.
[37] S. Kobtsev, S. Kukarin, Y. Fedotov, Ultra-low repetition rate mode-locked fiber laser with high-energy pulses, Opt. Express 16 (2008) 21936–21941.
[38] S.M. Kobtsev, S.V. Kukarin, S.V. Smirnov, Y.S. Fedotov, High-energy mode-locked all-fiber laser with ultralong resonator, Laser Phys. 20 (2010) 351–356.
[39] A. Ivanenko, S. Turitsyn, S. Kobsev, M. Dubov, Mode-locking in 25-km fiber laser, European Conference on Optical Communication (ECOC), 1–3, (2010).
[40] J.R. Kelleher, J.C. Travers, Z. Sun, A.G. Rozhin, A.C. Ferrari, S.V. Popov, J.R. Taylor, Nanosecond-pulse fiber lasers mode-locked with nanotubes, Appl. Phys. Lett. 95 (2009) 111108.
[41] Y. Senoo, N. Nishizawa, Y. Sakakibara, K. Sumimura, E. Itoga, H. Kataura, K. Itoh, Ultralow-repetition-rate, high-energy, polarization-maintaining, Er-doped, ultrashort-pulse fiber laser using single-wall-carbon-nanotube saturable absorber, Opt. Express 18 (2010) 20673–20680.
[42] L. Chen, M. Zhang, C. Zhou, Y. Cai, L. Ren, Z. Zhang, Ultra-low repetition rate linear-cavity erbium-doped fiber laser modelocked with semiconductor saturable absorber mirror, El. Lett. 45 (2009) 731–733.
[43] X. Tian, M. Tang, P.P. Shum, Y. Gong, C. Lin, S. Fu, T. Zhang, High-energy laser pulse with a submegahertz repetition rate from a passively mode-locked fiber laser, Opt. Lett. 34 (2009) 1432–1434.
[44] M. Zhang, L.L. Chen, C. Zhou, Y. Cai, L. Ren, Z.G. Zhang, Mode-locked ytterbium-doped linear-cavity fiber laser operated at low repetition rate, Laser Phys. Lett. 6 (2009) 657.
[45] F. Ai, Z. Cao, X. Zhang, C. Zhang, B. Zhang, B. Yu, Passively mode-locked fiber laser with kilohertz magnitude repetition rate and tunable pulse width, Opt. Laser Technol. 43 (2011) 501–505.
[46] A. Zaviyalov, O. Egorov, R. Iliew, F. Lederer, Rogue waves in mode-locked fiber lasers, Phys. Rev. A 85 (2012) 013828.
[47] M. Baumgartl, J. Abreu-Afonso, A. Díez, M. Rothhardt, J. Limpert, A. Tünnermann, Environmentally stable picosecond Yb fiber laser with low repetition rate, Appl. Phys. B 111 (2013) 39–43.
[48] B.N. Nyushkov, V.I. Denisov, S.M. Kobtsev, V.S. Pivtsov, N.A. Kolyada, A.V. Ivanenko, S.K. Turitsyn, Generation of 1.7-uJ pulses at 1.55 um by a self-mode-locked all-fiber laser with a kilometers-long linear-ring cavity, Laser Phys. Lett. 7 (2010) 661–665.
[49] B.N. Nyushkov, A.V. Ivanenko, S.M. Kobtsev, S.K. Turitsyn, C. Mou, L. Zhang, V.I. Denisov, V.S. Pivtsov, Gamma-shaped long-cavity normal-dispersion mode-locked Er-fiber laser for sub-nanosecond high-energy pulsed generation, Laser Phys. Lett. 9 (2012) 59–67.
[50] J.L. Dong, W.C. Xu, Z.C. Luo, A.P. Luo, H.Y. Wang, W.J. Cao, L.Y. Wang, Tunable and switchable dual-wavelength passively mode-locked fiber ring laser with high-energy pulses at a sub-100 kHz repetition rate, Opt. Commun. 284 (2011) 5719–5722.
[51] P. Grelu, W. Chang, A. Ankiewicz, J.M. Soto-Crespo, N. Akhmediev, Dissipative soliton resonance as a guideline for high-energy pulse laser oscillators, J. Opt. Soc. Am. B 27 (2010) 2336–2341.
[52] S.M. Kobtsev, S.V. Smirnov, Fiber lasers mode-locked due to nonlinear polarization evolution: golden mean of cavity length, Laser Phys. 21 (2011) 272–276.
[53] S.K. Turitsyn, Theory of energy evolution in laser resonators with saturated gain and non-saturated loss, Opt. Express 17 (2009) 11898.